



Virginia Commonwealth University
VCU Scholars Compass

Electrical and Computer Engineering Publications

Dept. of Electrical and Computer Engineering

2003

Stimulated emission and ultrafast carrier relaxation in AlGa_N/Ga_N multiple quantum wells

Ü. Özgür

Virginia Commonwealth University, Duke University, uozgur@vcu.edu

Henry O. Everitt

Duke University

Lei He

Virginia Commonwealth University

Hadis Morkoç

Virginia Commonwealth University, hmorkoc@vcu.edu

Follow this and additional works at: http://scholarscompass.vcu.edu/egre_pubs

 Part of the [Electrical and Computer Engineering Commons](#)

Özgür, Ü., Everitt, H.O., He, L., et al. Stimulated emission and ultrafast carrier relaxation in AlGa_N/Ga_N multiple quantum wells. *Applied Physics Letters*, 82, 4080 (2003). Copyright © 2003 AIP Publishing LLC.

Downloaded from

http://scholarscompass.vcu.edu/egre_pubs/71

This Article is brought to you for free and open access by the Dept. of Electrical and Computer Engineering at VCU Scholars Compass. It has been accepted for inclusion in Electrical and Computer Engineering Publications by an authorized administrator of VCU Scholars Compass. For more information, please contact libcompass@vcu.edu.

Stimulated emission and ultrafast carrier relaxation in AlGaN/GaN multiple quantum wells

Ümit Özgür and Henry O. Everitt^{a)}

Department of Physics, Duke University, Durham, North Carolina 27708

Lei He and Hadis Morkoç

Department of Electrical Engineering, Virginia Commonwealth University, Richmond, Virginia 23284

(Received 2 December 2002; accepted 9 April 2003)

Stimulated emission (SE) and ultrafast carrier relaxation dynamics were measured in two $\text{Al}_x\text{Ga}_{1-x}\text{N}/\text{GaN}$ multiple-quantum-well (MQW) structures, grown in a Ga-rich environment with $x=0.2$ and 0.3 , respectively. The threshold density for SE ($I_{\text{th}} \approx 100 \mu\text{J}/\text{cm}^2$) was found to be independent of x . Room-temperature, time-resolved, differential transmission measurements mapped the carrier relaxation mechanisms for above barrier energy excitation. Photoexcited carriers are observed to relax into the QWs in < 1 ps, while carrier recombination times as fast as 30 ps were measured. For excitation above I_{th} , SE is shown to deplete carriers in the barriers through a cascaded refilling of the QW state undergoing SE. Similar behavior is seen in an $\text{Al}_{0.3}\text{Ga}_{0.7}\text{N}/\text{GaN}$ MQW grown with a N-rich atmosphere, but the relaxation phenomena of all AlGaN MQWs are significantly faster than observed in InGaN MQWs of similar structure. © 2003 American Institute of Physics. [DOI: 10.1063/1.1581385]

Recent advances in the growth of group-III nitride heterostructures have made it possible to manufacture efficient green, blue, and ultraviolet emitters and detectors.^{1,2} AlGaN-based structures are promising for deep-UV emitter and detector applications.³ Carrier dynamics in such device structures are beginning to be understood through the use of high-power, short-pulse, regenerative, and optical parametric amplifiers.⁴⁻⁶ In addition to several studies of stimulated emission (SE)^{7,8} and time-resolved photoluminescence,⁹⁻¹¹ there have been only a few pump/probe studies¹² on AlGaN/GaN multiple-quantum-well (MQW) structures. In this paper, SE is explored in $\text{Al}_x\text{Ga}_{1-x}\text{N}/\text{GaN}$ MQW structures with differing barrier heights ($x=0.2, 0.3$) and MQW growth environments (Ga-rich, N-rich). SE threshold power densities are observed to be insensitive to these parameters, and ultrafast, time-resolved, differential transmission (TRDT) measurements of the carrier dynamics reveal why. Here, we report an extensive study of ultrafast carrier relaxation in AlGaN based MQWs using nondegenerate pump/probe techniques.

Two undoped AlGaN/GaN MQW samples were grown on *c*-plane sapphire by molecular-beam epitaxy under Ga-rich conditions. Both samples have ~ 30 -nm-thick AlN buffer layers. The 20% sample consists of 15 periods of 9-nm/3-nm $\text{Al}_{0.20}\text{Ga}_{0.80}\text{N}/\text{GaN}$ QWs grown on a ~ 0.7 - μm -thick $\text{Al}_{0.28}\text{Ga}_{0.72}\text{N}$ buffer layer, and is capped with a 100-nm-thick $\text{Al}_{0.28}\text{Ga}_{0.72}\text{N}$ layer. The 30% sample consists of 15 periods of 9-nm/3-nm $\text{Al}_{0.30}\text{Ga}_{0.70}\text{N}/\text{GaN}$ QWs grown on a ~ 0.7 - μm -thick $\text{Al}_{0.36}\text{Ga}_{0.64}\text{N}$ buffer layer, and is capped with a 100-nm-thick $\text{Al}_{0.36}\text{Ga}_{0.64}\text{N}$ layer. The buffer and cap layer Al compositions are determined by x-ray measurements in these samples together with samples containing only the individual layers such as the buffer layer. An AlGaN MQW sample, similar to the 30% sample except that the

MQW region was grown in N-rich conditions, was also studied to see how the recombination characteristics and emission efficiency depended on growth conditions. Unless otherwise indicated, the data refer to the Ga-rich samples.

Photoluminescence (PL) was obtained at room temperature using both cw, low-intensity, 4.14-eV excitation from a 300-W Xe lamp and time-integrated (TI), high-energy density ($\sim 50 \mu\text{J}/\text{cm}^2$), 4.08-eV excitation from a pulsed (~ 100 -fs) laser (Fig. 1). Both Ga-rich MQW samples show two distinct cw-PL emission peaks: at 3.43 and 3.74 eV for the 20% sample, and at 3.46 and 3.83 eV for the 30% sample. The lower-energy peaks are the main PL from the QWs, and the higher-energy peaks are the PL from the cap and buffer layers. Although QW emission from the N-rich MQW (3.49 eV) occurs at nearly the same energy as the 30% Ga-rich MQW, emission from the QWs is relatively weaker in the N-rich sample. For all samples, TI PL from spontaneous emission (SPE) blueshifted with increasing pump pulse intensity (Fig. 1) due to band filling and piezoelectric field screening^{13,14} by the increasing number of photoexcited carriers. No PL is observed from the barrier layers.

The cw PL excitation (cw-PLE) measurements were also performed at room temperature using the 300-W Xe lamp and detection energies corresponding to the MQW cw-PL peaks. The peaks of the broad PLE signals, at 3.98 eV for the 20% sample and at 4.10 eV for the 30% sample, were related to the absorption in the cap and buffer layers. Other absorption features, observed approximately 200 meV lower in energy at 3.78 and 3.89 eV, revealed the three-dimensional barrier band edges for the 20% and 30% samples, respectively. The corresponding effective QW band edges, defined as the energy for which the PLE magnitude reduced to half the value of the lowest energy shoulder, occurred at 3.55 and 3.60 eV. The PLE of the N-rich sample was nearly identical to the 30% Ga-rich sample, except that the absorption by a higher-lying confined MQW state (3.75 eV) was more prominent. (Simple calculations indicated that no such state

^{a)}Electronic mail: everitt@aro.arl.army.mil

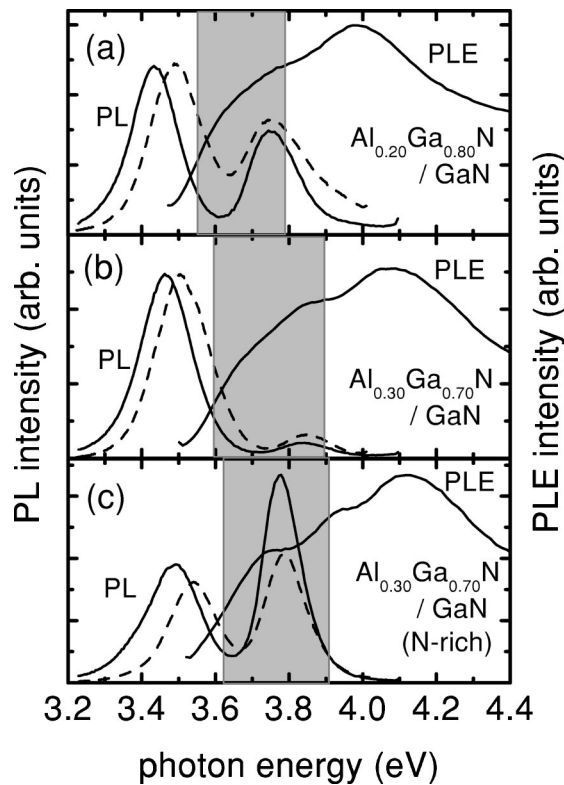


FIG. 1. Room-temperature cw-PL using a Xe lamp source (solid), time-integrated, below ($\sim 50 \mu\text{J}/\text{cm}^2$) I_{th} , pulsed-PL (dashed), and PLE for the (a) 20% Ga-rich, (b) 30% Ga-rich, and (c) 30% N-rich AlGaIn/GaN MQW samples. The regions between the barrier and the effective QW band edge energies are shaded.

exists in the 20% sample.) The large ($\sim 130 \text{ meV}$), Stokes-like shifts from the effective QW band edge to the cw-PL were due to the large strain-induced piezoelectric fields present in the QWs.

At moderate pump densities ($\sim 100 \mu\text{J}/\text{cm}^2$), SE is observed from all samples. The incident 4.08-eV pulsed excitation was 45° to the surface normal, and the TI-PL was measured normal to the surface as a function of average pump energy density. The excitation density-dependent, spectrally integrated TI-PL data (Fig. 2) indicates that SE threshold densities (I_{th}) were similar: $110 \mu\text{J}/\text{cm}^2$ for the 20% sample and $100 \mu\text{J}/\text{cm}^2$ for the 30% sample. The Al-

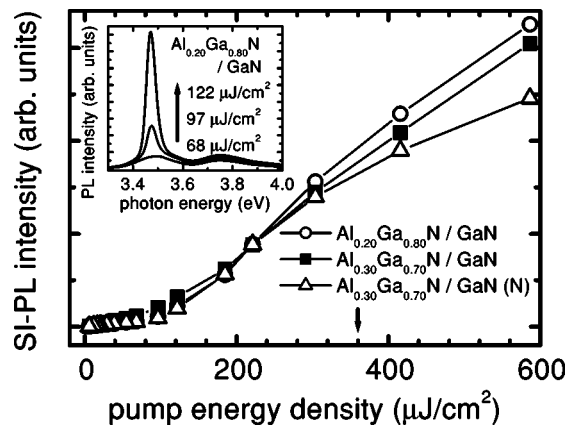


FIG. 2. Spectrally integrated PL intensity for the AlGaIn/GaN MQW samples at different excitation densities. The arrow shows the pump energy density used for the TRDT measurements. (N) indicates the N-rich sample. The inset shows the TI-PL below and above the I_{th} for the 20% sample.

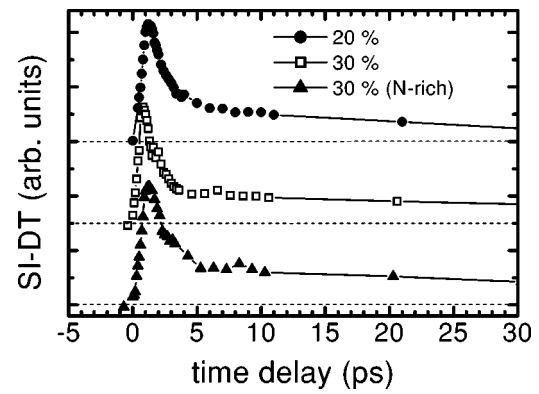


FIG. 3. SI-TRDT for the 20% Ga-rich, 30% Ga-rich, and 30% N-rich samples.

GaN MQW sample grown under N-rich conditions also had $I_{\text{th}} \approx 100 \mu\text{J}/\text{cm}^2$. The SE feature for all samples emerged from the QW SPE emission feature, indicating that the SE originates from the QW confined states (inset, Fig. 2). Although narrower than the SPE component, the linewidths of the SE feature increased due to power broadening as the excitation density increased.

To investigate the carrier dynamics in the presence of SE, nondegenerate, TRDT spectroscopy was applied at room temperature. The subpicosecond experimental technique, involving a wavelength tunable, ~ 100 -fs pump, and a pulsed broadband continuum probe, has been described elsewhere.⁴

To examine the relaxation of the total population of carriers, TRDT signals are spectrally integrated (SI) over all energies where photoexcited carriers were observed (Fig. 3). For an excitation energy of 3.93 eV, above the barrier band edge and below the cap and buffer layer band gaps, all samples show an initial fast decay followed by a slower relaxation for densities ($\sim 360 \mu\text{J}/\text{cm}^2$) above I_{th} . SI-TRDT data were fit by a biexponential decay function, $F e^{-t/\tau_F} + S e^{-t/\tau_S}$, where τ_F and τ_S are the decay constants, and F and S are the magnitudes, for the fast and slow decaying components, respectively (Table I). For all samples, the magnitude (F) and decay rate ($1/\tau_F$) of the fast component were found to increase with increasing excitation density, indicating that the fast feature is caused by the accelerated relaxation of carriers through SE. By contrast, the size and decay rate of the slow component were excitation density-independent and reflect the effects of recombination. However, the fractional strengths [$\equiv F/(F+S)$] for all samples were large, indicating that the majority of photoexcited carriers relax through SE.

TABLE I. Decay characteristics for SI-TRDT data.

Sample	Pump density ($\mu\text{J}/\text{cm}^2$)	τ_F (ps)	τ_S (ps)	$F/(F+S)$	
Ga-rich	20%	360	1.18 ± 0.04	29 ± 2	0.72
		270	1.49 ± 0.11	34 ± 2	0.66
		140	1.49 ± 0.36	32 ± 9	0.59
30%	360	1.06 ± 0.08	37 ± 6	0.72	
N-rich	30%	360	1.48 ± 0.12	55 ± 5	0.70
		280	1.55 ± 0.21	50 ± 4	0.52
		280	1.55 ± 0.21	50 ± 4	0.52

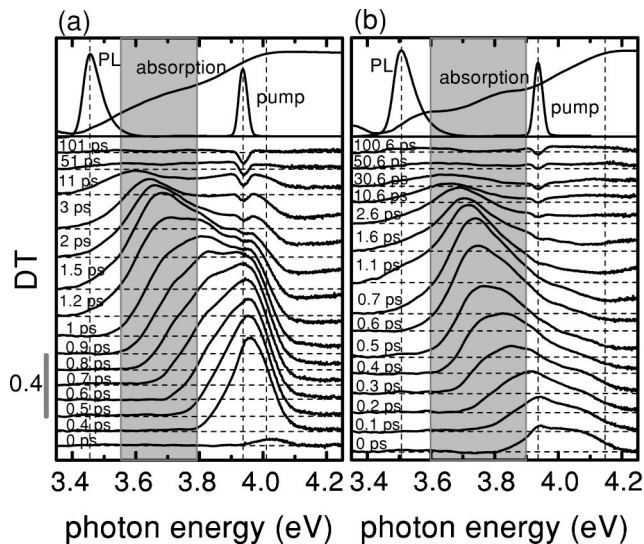


FIG. 4. SR-TRDT for the (a) 20% and (b) 30% Ga-rich samples. Shaded regions show the states between the barrier and the effective QW band edges. The vertical bars on the sides indicate a DT magnitude of 0.4.

Spectrally-resolved TRDT (SR-TRDT) data for the Ga-rich 20% and 30% samples at excitation densities above I_{th} further elucidates the carrier redistribution and relaxation processes (Fig. 4). For both samples, photoexcited carriers quickly relax within the barriers and the QWs. The 20% sample is excited farther from the barrier band edge than the 30% sample, so the peak of the carrier distribution reaches the band edge more slowly (0.5 ps, 0.2 ps). Carrier capture into the QWs occurs in ~ 0.5 ps, but notice that the decay occurs asymmetrically with energy. Carrier capture causes the blue side of the carrier distribution to decay quickly (< 3 ps), while recombination, which governs the decay of the red edge, proceeds more slowly (< 50 ps). The SE in the MQWs accelerates the decay of the blue side by removing carriers from the corresponding QW states, causing carriers at higher energies to cascade down and refill these SE-emptied states. The fast decay feature in the SI-TRDT (Fig. 3) is caused by this combination of SE and capture, while the slow decay feature is caused by recombination. Almost no photoexcited carriers are left after 100 ps.

A few additional observations from the SR-TRDT data deserve mention. First, the 20% sample was excited at an energy (3.93 eV) nearer the cap and buffer layer band gap (3.98 eV) than the 30% sample. As a result, a larger number of carriers are photogenerated in these layers by way of the ac Stark effect and two-photon absorption, effects which are known to increase as the detuning is decreased.⁵ The carrier distribution is therefore counterintuitively broader for the 20% sample (380 meV) than for the 30% sample (250 meV) because of carriers trapped in these higher energy cap and buffer states. These trapped carriers are unable to decay into the QWs and are energetically unavailable to participate in the refilling process required to sustain SE. Second, the N-rich sample SR-TRDT data (not shown) behaves in a similar manner to the 30% Ga-rich sample, but with slightly lower decay constants. The higher-energy confined MQW state at 3.8 eV is more pronounced in the N-rich sample, but its only role in relaxation is to provide an additional pathway

for relaxing carriers. Nevertheless, the SE threshold, the SE rate, the capture rate, and the recombination rate are found to be rather insensitive to barrier height and Ga-rich or N-rich growth conditions. However, it is worth noting that previous measurements of recombination at room temperature observed greater growth-dependent results than reported here. For example, recombination lifetimes between 180 ps and 1 ns have been measured for AlGaIn/GaN MQWs grown on GaN buffer layers.^{9,15}

It is instructive to compare the relaxation of carriers in these AlGaIn MQWs with InGaIn MQWs of similar depth, width, and excitation density.^{4,16} In both cases, carrier capture occurs in < 1 ps, and SE removes carriers from the barriers on the blue side of the carrier distribution through a cascaded refilling of emptied QW states. However, the fast, SE-accelerated decay in AlGaIn MQWs occurs more than twice as fast as in InGaIn MQWs for similar excitation intensities. More importantly, recombination times are an order of magnitude faster in AlGaIn MQWs^{9,15} than in InGaIn MQWs.^{4,16} It has been suggested that nonradiative recombination plays a much greater role in AlGaIn,^{10,11,17-19} but the relative rates for radiative and nonradiative recombination could not be ascertained with the data presented here.

The Duke portion of this work was supported by ARO grant DAAG55-98-D-0002-0007, and the VCU portion was funded by AFOSR MURI through University of Michigan, and by grants from ONR, NSF, and AFOSR.

- ¹ S. Nakamura and G. Fasol, *The Blue Laser Diode* (Springer, Berlin, 1997), and references therein.
- ² H. Morkoç, *Nitride Semiconductors and Devices* (Springer, Berlin, 1999).
- ³ H. Hirayama, Y. Enomoto, A. Kinoshita, A. Hirata, and Y. Aoyagi, *Appl. Phys. Lett.* **80**, 37 (2002).
- ⁴ Ü. Özgül, H. O. Everitt, S. Keller, and S. P. DenBaars, *Appl. Phys. Lett.* **82**, 1416 (2003).
- ⁵ Ü. Özgül and H. O. Everitt, <http://xxx.lanl.gov/abs/cond-mat/0210214>
- ⁶ Y. Kawakami, Y. Narukawa, K. Omae, S. Fujita, and S. Nakamura, *Appl. Phys. Lett.* **77**, 2151 (2000).
- ⁷ R. Cingolani, G. Coli, R. Rinaldi, L. Calcagnile, H. Tang, A. Botchkarev, W. Kim, A. Salvador, and H. Morkoç, *Phys. Rev. B* **56**, 1491 (1997).
- ⁸ T. J. Schmidt, X. H. Yang, W. Shan, J. J. Song, A. Salvador, W. Kim, Ö. Aktas, A. Botchkarev, and H. Morkoç, *Appl. Phys. Lett.* **68**, 1820 (1996).
- ⁹ K. C. Zeng, J. Li, J. Y. Lin, and H. X. Jiang, *Appl. Phys. Lett.* **76**, 864 (2000).
- ¹⁰ K. C. Zeng, J. Li, J. Y. Lin, and H. X. Jiang, *Appl. Phys. Lett.* **76**, 3040 (2000).
- ¹¹ E.-J. Shin, J. Li, J. Y. Lin, and H. X. Jiang, *Appl. Phys. Lett.* **77**, 1170 (2000).
- ¹² A. Shikanai, T. Deguchi, T. Sota, T. Kuroda, A. Takeuchi, S. Chichibu, and S. Nakamura, *Appl. Phys. Lett.* **76**, 2511 (2000).
- ¹³ R. Cingolani, A. Botchkarev, H. Tang, H. Morkoç, G. Traetta, G. Coli, M. Lomascio, A. DiCarlo, F. DellaSala, and P. Lugli, *Phys. Rev. B* **61**, 2711 (2000).
- ¹⁴ A. Kinoshita, H. Hirayama, P. Riblet, M. Ainoya, A. Hirata, and Y. Aoyagi, *MRS Internet J. Nitride Semicond. Res.* **5S1**, W11.32 (2000).
- ¹⁵ J. C. Harris, T. Someya, K. Hoshino, S. Kako, and Y. Arakawa, *Phys. Status Solidi A* **180**, 339 (2000).
- ¹⁶ S. Chichibu, T. Sota, K. Wada, and S. Nakamura, *J. Vac. Sci. Technol. B* **16**, 2204 (1998).
- ¹⁷ M. Wraback, F. Semendy, H. Shen, U. Chowdhury, D. J. H. Lambert, M. M. Wong, and R. D. Dupuis, *Phys. Status Solidi A* **188**, 807 (2001).
- ¹⁸ M. Gallart, A. Morel, T. Taliercio, P. Lefebvre, B. Gil, J. Allègre, H. Mathieu, N. Grandjean, J. Massies, I. Grzegory, and S. Porowsky, *Mater. Sci. Eng., B* **82**, 140 (2001).
- ¹⁹ Y.-H. Cho, G. H. Gainer, J. B. Lam, J. J. Song, W. Yang, and W. Jhe, *Phys. Rev. B* **61**, 7203 (2000).